Study of the 6Li + p $ \rightarrow$ 3He + 4He reaction in inverse kinematics

Article *in* European Physical Journal A · July 2015

DOI: 10.1140/epja/i2015-15086-y

Eur. Phys. J. A (2015) **51**: 86
DOI 10.1140/epja/i2015-15086-y

THE EUROPEAN
PHYSICAL JOURNAL A

Regular Article – Experimental Physics

Study of the ^{6}Li + p → ^{3}He + ^{4}He reaction in inverse kinematics

Ch. Betsou[1], A. Pakou[1,a], F. Cappuzzello[2,3], L. Acosta[4,5], C. Agodi[2], X. Aslanoglou[1], D. Carbone[2], M. Cavallaro[2], A. Di Pietro[2], J.P. Fernández-García[2], P. Figuera[2], M. Fisichella[2], A. Foti[3,5], N. Keeley[6], G. Marquinez-Duran[7], I. Martel[7], M. Mazzocco[8,9], N.G. Nicolis[1], D. Pierroutsakou[10], K. Rusek[11], O. Sgouros[1], V. Soukeras[1], E. Stiliaris[12], E. Strano[8,9], and D. Torresi[8,9]

[1] Department of Physics and HINP, The University of Ioannina, 45110 Ioannina, Greece
[2] INFN Laboratori Nazionali del Sud, via S. Sofia 62, 95125, Catania, Italy
[3] Dipartimento di Fisica e Astronomia, Universita di Catania, via S. Sofia 64, 95125, Catania, Italy
[4] Instituto de Fisica, Universidad Nacional Autonoma de Mexico, Mexico Distrito Federal 01000, Mexico
[5] INFN - Sezione di Catania, via S. Sofia 64, 95125, Catania, Italy
[6] National Centre for Nuclear Research, ul. Andrzeja Sołtana 7, 05-400 Otwock, Poland
[7] Departamento di Fisica Aplicada, Universidad de Huelva, E-21071, Huelva, Spain
[8] Departimento di Fisica e Astronomia, Universita di Padova, via Marzolo 8, I-35131, Padova, Italy
[9] INFN - Sezione di Padova, via Marzolo 8, I-35131, Padova, Italy
[10] INFN - Sezione di Napoli, via Cinthia, I-80126, Napoli, Italy
[11] Heavy Ion Laboratory, University of Warsaw, ul. Pasteura 5a, 02-093, Warsaw, Poland
[12] Institute of Accelerating Systems and Applications and Department of Physics, University of Athens, Greece

Received: 11 May 2015 / Revised: 22 June 2015
Published online: 20 July 2015 –
Communicated by N. Alamanos

Abstract. Angular distribution measurements were performed for the ^{6}Li + p → ^{3}He + ^{4}He reaction in inverse kinematics at incident energies of 2.7, 3.3, 4.2 and 4.8 MeV/u. The detection of both recoils (^{3}He and ^{4}He) over the laboratory angle range $\theta_{\text{lab}} = 16°$ to $34°$ allowed the determination of the angular distribution over a wide angular range in the center-of-mass frame ($\theta_{\text{c.m.}} \sim 40°$ to $140°$). The results clarify inconsistencies between existing data sets and are consistent with compound nucleus model calculations.

1 Introduction

The significance of the ^{6}Li(p, ^{3}He)^{4}He reaction has been demonstrated for a long time in several experimental studies. These are related not only to studies of controlled thermonuclear reactors based on the use of advanced fusion fuels [1–3], but also to fundamental astrophysical problems like the understanding of Big Bang nucleosynthesis and "lithium depletion", either in the sun or in other galactic stars [4–7].

The above reaction is reconsidered in this work as a complementary study to our recent measurements of elastic scattering and breakup modes [8] with the MAGNEX spectrometer [9–11]. The latter is part of a systematic continuing research program of our groups, relative to the optical potential at near-barrier energies with weakly bound projectiles. In this respect the present results will be used in future work on a global understanding of the optical potential and relevant reaction mechanisms. Last but not least, these data also serve to clarify the experimental situation at these energies, as several inconsistencies occur in previous results [12–21]. Our theoretical analysis will focus on the reaction mechanism in a compound nucleus framework.

[a] e-mail: apakou@cc.uoi.gr

2 Experimental details and data reduction

The experiment was performed at the Istituto Nazionale di Fisica Nucleare, Laboratori Nazionali del Sud (INFN-LNS) in Catania, Italy. Beams of ^{6}Li^{3+} were accelerated by the SMP13 tandem to energies of 16, 20, 25 and 29 MeV and impinged on a $\sim 300\,\mu$g/cm^2 CH$_2$ target. In the first phase of the experiment the elastically scattered lithium ions, directed only at forward angles, were momentum analyzed by the MAGNEX spectrometer [9–11] and the corresponding angular distributions were reported in ref. [8]. In the second phase of the experiment a breakup measurement, to be reported later [22], was undertaken. In this measurement the ^{4}He breakup fragment, also directed at forward angles, was momentum analyzed by MAGNEX and recorded in coincidence with the ^{2}H fragment, detected by a silicon detector at 5°. In both phases of the

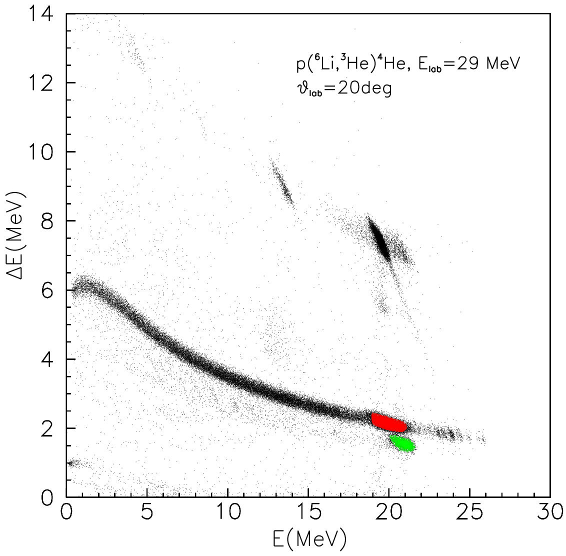

Fig. 1. Two-dimensional ΔE-E spectrum collected at $\theta_{\rm lab} = 20°$ for the ^{6}Li + p → ^{3}He + ^{4}He reactions at a bombarding energy of 29.0 MeV. The green spot corresponds to ^{3}He and the red to ^{4}He.

experiment a parallel measurement of the angular distribution of the ^{6}Li + p → ^{4}He + ^{3}He reaction, reported herein, was performed using one telescope of the DINEX array [23]. The telescope was set at a distance of 15.5 cm from the target, covering an angular range of $\theta_{\rm lab} = 16°$ to $34°$. The ΔE stage of the telescope was a DSSSD silicon detector, 48 μm thick, with an active area of $5 \times 5\,\rm cm^2$ and 16 strips per side. The E stage was a silicon pad, 530 μm thick. The solid angle of each strip was determined by an elastic scattering measurement performed with a gold foil target at the lowest energies, where the scattering can be considered as pure Rutherford. The gold foil measurements, together with measurements performed with a carbon foil 240 μg/cm^2 thick, were used for energy calibration purposes. The carbon target measurements were also used to estimate the background due to carbon in our CH_2 target.

An angular distribution measurement was performed at each energy by detecting both reaction products, ^{4}He and ^{3}He. It was thus possible to span a wide angular range in the center of mass frame ($\theta_{\rm c.m.} = 40°$ to $140°$, corresponding to $\theta_{\rm lab} = 16°$ to $34°$). The ^{3}He ejectiles were well resolved via the ΔE-E technique, as can be seen from fig. 1, where a two-dimensional spectrum is shown (green spot). On the other hand, while the ^{4}He products were also well resolved with the same technique, the ^{4}He peak from the two-body reaction under study (red spot in fig. 1) sat on top of a continuous background. This originated from the ^{6}Li projectile breakup on hydrogen and carbon as well as from fusion reactions on the carbon of the CH_2 target. This background was estimated by placing windows to the left and right of the "peak" in the two-dimensional spectrum. Cross sections obtained in the overlapping angular regions (see table 1) where data exist from both reaction products (^{4}He and ^{3}He) are in

Table 1. Angular range in the center of mass frame, spanned by detecting ^{3}He and ^{4}He reaction products. The overlapping angular range is also indicated where it exists.

	$\theta_{\rm c.m.}$ (deg)		
$E_{\rm lab}$ (MeV)/isotope	^{3}He	^{4}He	Overlap
29.0	89–138	51–103	89–103
25.0	96–140	50–100	96–100
20.0	97–141	47–103	97–103
16.0	101–143	45–94	–

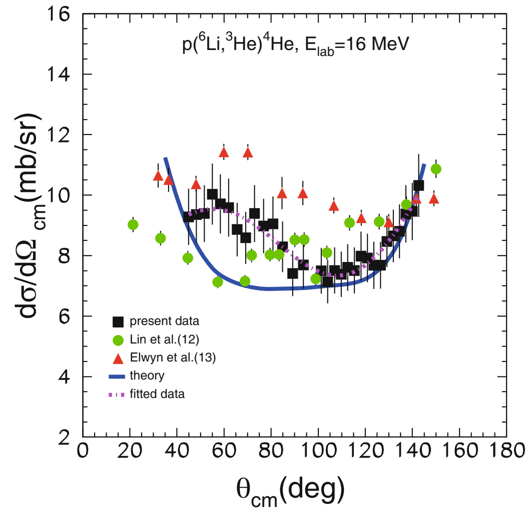

Fig. 2. Present angular distribution data for the ^{6}Li + p → ^{3}He + ^{4}He reaction at a bombarding energy of 16 MeV (2.7 MeV/u) are compared with previous data [12,13] and with compound calculations performed with the code MECO [33].

agreement to within 5%, giving support to the accuracy of the background subtraction. Normalization of the data was effected via the integrated beam charge, recorded in the Faraday cup. The accuracy of the beam charge integration was tested in the first phase of the experiment via the Rutherford scattering of ^{6}Li on hydrogen recorded in MAGNEX [8]. The assigned error in the differential cross sections due to statistics is less than 0.3% and the rest is due to a 5% error in the estimation of the target thickness, 5% in the measured integrated beam charge and 7% due to the solid angle measurement. The results at the four energies are presented in figs. 2, 3, 4 and 5 and are compared with previous measurements. At the two higher energies the agreement with the Gould *et al.* data [18] is good, at 20 MeV the agreement worsens, while at 16 MeV the inconsistency between the two existing sets of data of Elwyn *et al.* [13] and Lin *et al.* [12] is partly clarified by the present results. The new data at backward angles seem to agree well with the Lin *et al.* data, while at forward angles they seem to be located between the previous two measurements.

Finally, our differential cross sections were fitted to a sum of Legendre polynomials ($\sum_L \mathrm{B}_L \mathrm{P}_L(\cos\theta)$) with five terms. Variations of the fits with four or seven terms do

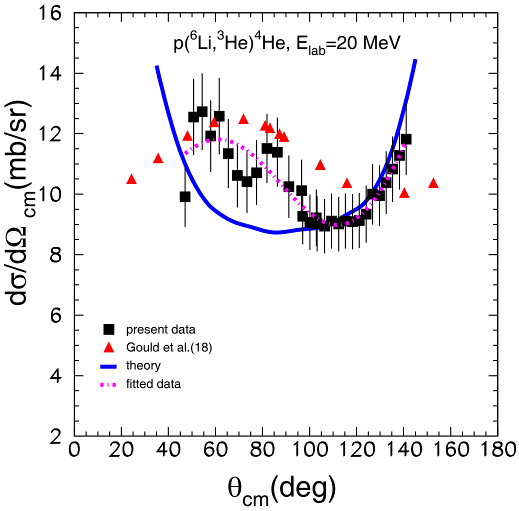

Fig. 3. As in fig. 2, but for a bombarding energy of 20 MeV (3.3 MeV/u). The previous data are from ref. [18].

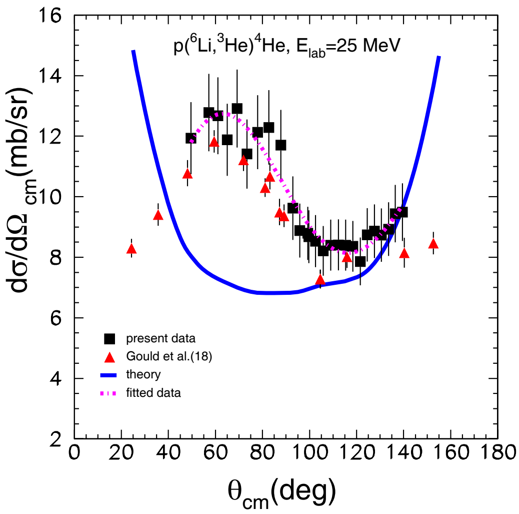

Fig. 4. As in fig. 2, but for a bombarding energy of 25 MeV (4.2 MeV/u). The previous data are from ref. [18].

not change appreciably the reaction cross section results, not more than 10%. Although a change in the shape at the more forward and backward angles does occur, this cannot be verified as the data are limited to the angular range between $\theta_{\text{c.m.}} = 40°$ to $140°$. The fits are represented in figs. 2, 3, 4 and 5 by dot-dashed lines. The resulting reaction cross sections for the $^6\text{Li}+\text{p} \rightarrow {}^3\text{He}+{}^4\text{He}$ reaction are included in table 2 (the mean of the three fits with the deviation of the mean) and are shown as a function of energy in fig. 6. Previous measurements [7,12,13,16–21] between 2 to 5 MeV/u are also displayed on fig. 6, and are compared with our results. The new results reveal previous inconsistencies and combined with the Lin *et al.* and Tumino *et al.* data [7,12] could indicate the possible presence of a broad

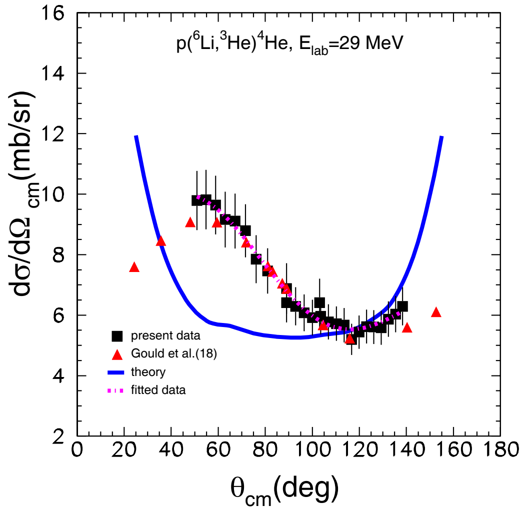

Fig. 5. As in fig. 2, but for a bombarding energy of 29 MeV (4.8 MeV/u). The previous data are from ref. [18].

Table 2. Cross sections for the $^6\text{Li}+\text{p} \rightarrow {}^3\text{He}+{}^4\text{He}$ reaction: present measurement, $\sigma^{\text{pres}}_{\text{meas}}$; calculation of compound production of ^{3}He and ^{4}He with the MECO code, σ_{MECO}; and the absorption cross section ($\sigma_{\text{tot}} - \sigma_{\text{break}}$) from CDCC calculations, σ_{CDCC}, [8].

E_{lab} (MeV)	$\sigma^{\text{pres}}_{\text{meas}}$ (mb)	σ_{MECO} (mb)	σ_{CDCC} (mb)
29.0	95 ± 2	90	110
25.0	131 ± 6	114	133
20.0	140 ± 8	145	162
16.0	111 ± 2	114	131

resonance at $E_p = 3.7$ MeV. This resonance is suggested for the first time. It should be noted that the Jeronymo *et al.* and Abramovich *et al.* results [17,19] appearing in fig. 6 are evaluated cross sections and not original experimental data. From the comparison it is obvious that the evaluation is valid only at the larger energies above 3 MeV.

3 Theoretical framework

Absorption cross sections were determined as follows. The experimental elastic scattering data, $^6\text{Li}+\text{p} \rightarrow {}^6\text{Li}+\text{p}$ [8], were reproduced in a Continuum Discretized Coupled Channel (CDCC) calculation framework. Details of the calculations can be found in ref. [8], while we give here just the points pertinent to this work. An $\alpha + d$ cluster model of ^{6}Li was adopted, with all the parameters of the model including continuum discretization and truncation described in detail in ref. [24]. The 3^+ resonance was taken into account and was treated as a momentum bin with a width of 0.1 MeV. The central parts of the $^6\text{Li} + p$ entrance channel potentials were derived as previously [25] from empirical $p+\alpha$ and $p+d$ optical potentials by means

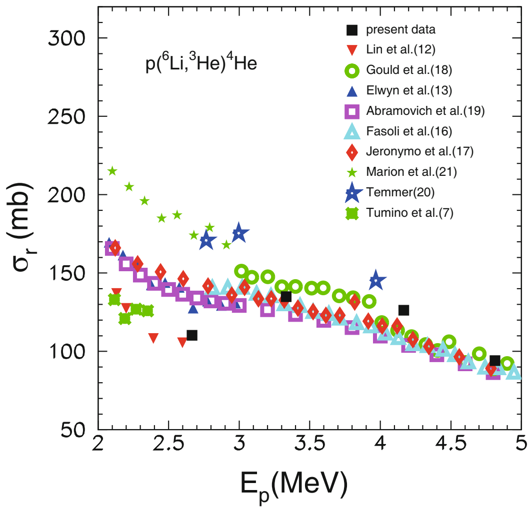

Fig. 6. Present reaction cross section measurements as a function of energy, designated by the boxes, compared with previous values [7,12,13,16–21]. It should be noted that the data of refs. [17,19] are evaluated data and not original experimental data.

of the Watanabe single-folding method. The empirical potentials were obtained from previous $p+d$ and $p+\alpha$ elastic scattering studies at $E = 2.52$ to $5\,\mathrm{MeV}/u$ [26–32]. These $p+d$ and $p+\alpha$ elastic scattering data were fitted by simple volume Woods-Saxon form factors for both real and imaginary parts for the $p+\alpha$ system and a real volume and a surface imaginary term for the $p+d$ system. In this way total reaction cross sections and breakup cross sections were determined. Further, absorption cross sections were calculated as the differences between total reaction and breakup cross sections. The results are included in table 2. It is obvious that the measured values exhaust most of the absorption cross section, indicating that the most prominent reaction in this energy range is the one under study. Subsequently, the present data were compared with a compound mechanism framework.

The compound nucleus decay was calculated with the equilibrium statistical model of nuclear reactions. For this purpose, the statistical model Monte Carlo code MECO (*M*ultisequential *E*vaporation *CO*de) was employed [33]. The code treats asymmetric mass divisions involving nucleon emission up to completely symmetric ones in a unified framework according to a generalized Weisskopf evaporation formalism [34,35]. The only input parameters introduced into the code were the above mentioned absorption cross sections. An excitation energy spread consistent with the beam energy loss through the target, which was less than 2.5%, was taken into account. No discrete structure was considered in the level schemes of the participating nuclei. Level densities were calculated in a Fermi gas model adopting an energy-independent level density constant $\alpha = A/8$. Variations of the level density constant in the range $A/7.0$ to $A/9.0$ affect the ^{3}He production cross section by less than 1%. Our calculations take into account 7 particle decay modes involving n, ^{1}H, ^{2}H, ^{3}H, ^{3}He, ^{4}He and ^{5}He emission. Gamma decay is considered as a competing emission mode in the form of dipole $E1$ transitions with a Lorentzian strength function and parameters quoted in ref. [33]. Angular distributions of the emitted particles were calculated using orbital angular momentum values from the transmission coefficient array, responsible for the decay under consideration. The calculations predict exit channels involving $^3\mathrm{He} + {}^4\mathrm{He}$ and $^1\mathrm{H} + {}^6\mathrm{Li}$ with a cross section ratio of $\sigma(^3\mathrm{He})/\sigma(^1\mathrm{H}) \sim 7$, 9, 6 and 4.5 for projectile energies of 16, 20, 25 and 29 MeV, respectively. At the highest energy the $^1\mathrm{H} + {}^2\mathrm{H} + {}^4\mathrm{He}$ channel has just opened.

At each bombarding energy ^{3}He angular distributions, plotted as the solid curves in figs. 2, 3, 4, and 5, were constructed by sorting the Monte Carlo events of correlated $^3\mathrm{He} + {}^4\mathrm{He}$ pairs. The angular distributions show the anisotropy expected for compound nucleus decay. At backward angles the agreement with the present data is very good, indicating the strong presence of the compound mechanism and precluding the validity of the Elwyn *et al.* data [13] both in shape and intensity. However, comparing the theoretical predictions and the experimental data it is apparent that there is a broad peak centered at approximately $\theta_{\mathrm{c.m.}} = 50°$ that is not explained by the MECO compound calculations and which becomes more pronounced as the bombarding energy increases. This peak could be due to a direct reaction component. To test this hypothesis we carried out coupled reaction channels (CRC) calculations for the $^6\mathrm{Li}(p,{}^3\mathrm{He})^4\mathrm{He}$ reaction using the code FRESCO [36]. The calculations were loosely based on those of Werby *et al.* [37] and included the exchange mode: $^6\mathrm{Li}(p,{}^4\mathrm{He})^3\mathrm{He}$. The results were in rough qualitative agreement with the shape of the measured angular distributions although the peak was shifted to larger angles compared to the data (the calculated angular distributions also had pronounced peaks at $\theta_{\mathrm{c.m.}} = 0°$ and 180° where we do not have data). However, it was found that the results were very sensitive to details of the input to the calculations, particularly the exit channel $^3\mathrm{He}+{}^4\mathrm{He}$ optical potential, which are poorly known. Therefore it is not possible to come to a more definite conclusion than that a direct reaction contribution is a plausible explanation for the broad peak in the measured $^3\mathrm{He}+{}^4\mathrm{He}$ angular distributions.

4 Discussion and summary

Angular distribution measurements were performed in inverse kinematics for the $^6\mathrm{Li} + \mathrm{p} \to {}^4\mathrm{He} + {}^3\mathrm{He}$ reaction at 2.7, 3.3, 4.2 and $4.8\,\mathrm{MeV}/u$. Both reaction products were observed, allowing the determination of the angular distribution over a wide angular range ($\theta_{\mathrm{c.m.}} \sim 40°$ to 140°). The results clarified some of the inconsistencies in existing data sets and were compared with theoretical calculations for determining the reaction mechanism. It was found that the $^6\mathrm{Li} + \mathrm{p} \to {}^4\mathrm{He} + {}^3\mathrm{He}$ reaction exhausts almost all the absorption from the elastic channel, while it proceeds at least by 85% via a compound mechanism. Further, the excellent agreement of the compound model calculations with the data at backward angles, which take into account absorption cross sections extracted from the ^{6}Li + p elastic scattering channel support the interconsistency of all data recorded and analysed in this experiment. Last but not least we should mention the observation of a possible new broad resonance centered at $E_p \sim 3.7\,\mathrm{MeV}$.

We warmly acknowledge the TANDEM operator staff of LNS for the production and delivery of the ^{6}Li beams. The research leading to these results was partially funded by the European Union Seventh Framework Programme FP7/2007-2013 under Grant Agreement No. 262010-ENSAR.

References

1. J.L. Hirshfied, *Proceedings of the Review Meeting on Advanced-Fuel Fusion EPRIER-S36-SR* (Electric Power Research Institute, Palo Alto-California, 1977) p. 251.
2. J.R. McNally, Nucl. Fusion **11**, 187 (1971).
3. B.W. Hooten, M. Ivanovich, AERE Harwell Report No AERE-PR/NP18 (1972).
4. C. Rolfs, W.S. Rodney, *Cauldrons in the Cosmos* (University of Chicago Press, Chicago, IL, 1989).
5. C. Rolfs, R.W. Kavanagh, Nucl. Phys. A **455**, 179 (1986).
6. J. Cruz, H. Luis, M. Fonseca, Z. Fulop, G. Gyurky, F. Raiola, M. Aliotta, K.U. Kettner, A.P. Jesus, J.P. Ribeiro, F.C. Barker, C. Rolfs, J. Phys. G **35**, 014004 (2008).
7. A. Tumino, C. Spitaleri, L. Pappalardo, S. Cherubini, A. Del Zoppo, M. La Cognata, A. Musumarra, M.G. Pellegriti, R.G. Pizzone, A. Rinollo, S. Romano, S. Typel, Nucl. Phys. A **734**, 639 (2004).
8. V. Soukeras, A. Pakou, F. Cappuzzello, L. Acosta, C. Agodi, N. Alamanos, M. Bondi, D. Carbone, M. Cavallaro, A. Cunsolo, M. De Napoli, A. Di Pietro, J.P. Fernandez-Garcia, P. Figuera, M. Fisichella, A. Foti, N. Keeley, G. Marquinez-Duran, I. Martel, M. Mazzocco, D. Nicolosi, D. Pierroutsakou, K. Rusek, O. Sgouros, E. Stiliaris, E. Strano, D. Torresi, Phys. Rev. C **91**, 057601 (2015).
9. A. Cunsolo, F. Cappuzzello, M. Cavallaro, A. Foti, A. Khouaja, S.E.A. Orrigo, J.S. Winfield, L. Gasparini, G. Longo, T. Borello-Lewin, M.R.D. Rodrigues, M.D.L. Barbosa, C. Nociforo H. Petrascu, Eur. Phys. J. ST **150**, 343 (2007).
10. A. Cunsolo, F. Cappuzzello, A. Foti, A. Lazzaro, A.L. Melita, C. Nociforo, V. Shchepunov, J.S. Winfield, Nucl. Instrum. Methods A **484**, 56 (2002).
11. A. Cunsolo, F. Cappuzzello, A. Foti, A. Lazzaro, A.L. Melita, C. Nociforo, V. Shchepunov, J.S. Winfield, Nucl. Instrum. Methods A **481**, 48 (2002).
12. Lin Chia-Shou, Hou Wan-Shou, Wen Min, Chou Jen-Chang, Nucl. Phys. A **275**, 93 (1977).
13. A.J. Elwyn, R.E. Holland, C.N. Davids, L. Meyer-Schutzmeister, F.P. Mooring, W. Ray, Jr., Phys. Rev. C **20**, 1984 (1979).
14. K. Schenk, M. Morike, G. Staudt, P. Turek, D. Clement, Phys. Lett. B **52**, 36 (1974).
15. G.P. Johnston, D.G. Sargood, Nucl. Phys. A **224**, 349 (1974).
16. U. Fasoli, D. Toniolo, G. Zago, Phys. Lett. B **8**, 127 (1964).
17. J.M.F. Jeronymo, G.S. Mani, A. Sadeghi, Nucl. Phys. A **43**, 424 (1963).
18. C.R. Gould, R.O. Nelson, J.R. Williams, J.R. Boyce, Nucl. Sci. Eng. **55**, 267 (1974).
19. S.N. Abramovich, B.Ja. Guzhovskij, V.A. Zherebcov, A.G. Zvenigorodskij, Vop. At. Nauki i Tekhn., Ser. Yad. Konst. **4/58**, 17 (1984).
20. G.M. Temmer, in *Nuclear Reaction Mechanisms Conference, Padua 1962, Italy* (1962) page 1013.
21. J.B. Marion, G. Weber, F.S. Mozer, Phys. Rev. **104**, 1402 (1956).
22. V. Soukeras *et al.*, in preparation.
23. G. Marquinez-Duran, L. Acosta, R. Berjillos, J.A. Duenas, J.A. Labrador, K. Rusek, A.M. Sanchez-Benitez, I. Martel, Nucl. Instrum. Methods A **755**, 69 (2014).
24. K. Rusek, P.V. Green, P.L. Kerr, K.W. Kemper, Phys. Rev. C **56**, 1895 (1997).
25. K. Rusek, K.W. Kemper, R. Wolski, Phys. Rev. C **64**, 044602 (2001).
26. R. Sherr, J.M. Blair, H.R. Kratz, C.L. Bailey, R.F. Taschek, Phys. Rev. **72**, 662 (1947).
27. F. Lahlou, R.J. Slobodrian, P. Bricault, S.S. Dasgupta, R. Roy, C. Rioux, J. Phys. France **41**, 485 (1980).
28. D.C. Kocher, T.B. Clegg, Nucl. Phys. A **132**, 455 (1969).
29. A.S. Wilson, M.C. Taylor, J.C. Legg, G.C. Phillips, Nucl. Phys. **130**, 624 (1969).
30. K. Sagara, H. Oguri, S. Shimizu, K. Maeda, H. Nakamura, T. Nakashima, S. Morinobu, Phys. Rev. C **50**, 576 (1994).
31. G. Freier, E. Lampi, W. Sieator, J.H. Williams, Phys. Rev. **75**, 1345 (1949).
32. P.D. Miller, G.C. Phillips, Phys. Rev. **112**, 2043 (1958).
33. N.G. Nicolis, Int. J. Mod. Phys. E **17**, 1541 (2008).
34. V.F. Weiskopf, Phys. Rev. **52**, 195 (1937).
35. M.A. Preston, *Physics of the Nucleus*, Addisson-Wesley Publishing Company (Reading Massachusetts, Palo Alto, London, 1962).
36. I.J. Thompson, Comput. Phys. Rep. **7**, 167 (1988).
37. M.F. Werby, M.B. Greenfield, K.W. Keeper, D.L. McShan, S. Edwards, Phys. Rev. C **6**, 106 (1973).